

Miscibility and segmental mobility in hydrogen-bonded polymer blends

Thomas C. Gsell, Eli M. Pearce and T. K. Kwei*

Department of Chemistry and Department of Chemical Engineering, Polytechnic University, Brooklyn, New York 11201, USA

(Received 2 March 1990; revised 31 May 1990; accepted 31 May 1990)

Water vapour was used as a diffusional probe to study the interaction and segmental mobility in hydrogen-bonded polymer blends. Modified polystyrenes containing *p*-(hexafluoro-2-hydroxyisopropyl) groups as hydrogen-bond donors were blended with poly(methyl methacrylate) and two styrene-acrylonitrile copolymers. Interaction parameters, estimated from solubilities of water vapour in the blends, were negative in all cases. Positive excess volumes were found for several pairs and were believed to be the result of poor chain packing of styrene and methyl methacrylate or acrylonitrile segments, which were inherently immiscible with each other. In a number of blends, the diffusion coefficients were higher than the 'average' values for the component polymers. The deviation in diffusion coefficient was opposite in sign to the deviation in the activation energy of diffusion from its 'average' value. The residual activation energy was proportional to the excess volume. Furthermore, an excellent correlation was found between diffusion coefficient and specific free volume.

(Keywords: miscibility; hydrogen bonding; blends; diffusion of water vapour)

INTRODUCTION

A large number of miscible polymer blends reported in the recent literature contain copolymers. It has been shown in many cases that, although homopolymers A, B and C are immiscible with each other, AB copolymers of certain compositions can be miscible with homopolymer C. A generalized treatment of the 'copolymer' effect, including blends of two copolymers, has been derived with the use of mean-field theory¹⁻³. Many salient features of experimentally observed phase behaviour agree with theoretical predictions.

A second approach to miscibility enhancement relies on polymer modification to introduce groups capable of engaging in specific interaction with the counter-polymer⁴⁻⁸. It has been demonstrated in several cases that small amounts of interacting groups suffice to produce completely miscible systems^{4,5}. For example, polystyrene (PS) is immiscible with poly(methyl methacrylate) (PMMA); but when it is modified to contain 2-4% of *p*-hydroxystyrene or *p*-(hexafluoro-2-hydroxyisopropyl)styrene (HHIS) as comonomer units, hydrogen-bonding interaction between the hydroxyl and carbonyl groups renders the modified PS miscible with PMMA.

Although the modified polystyrenes are, by definition, also copolymers, the underlying molecular picture of segmental intermixing is different from that depicted by the mean-field theory. In these blends, hydrogen bonds bridge long sequences of different types of segments, which are inherently immiscible with each other, and the question may be asked as to the characteristics of segmental motion in these blends.

The use of small molecules as probes has generated valuable information^{9,10} about polymer-polymer inter-

action and segmental mobility. In the present study water vapour was used as the diffusional probe. Hydrogen-bonded blends were prepared from three modified polystyrenes (MPS), two copolymers of styrene and acrylonitrile (PSAN) and poly(methyl methacrylate) (PMMA). One PMMA/PSAN pair, three PMMA/MPS pairs and six PSAN/MPS pairs were studied. These pairs were known to be miscible and three blend compositions were prepared for each pair. The PMMA/PSAN pair is representative of the copolymer effect as the underlying cause for miscibility¹¹⁻¹⁴ and provides a reference point for comparison with hydrogen-bonded systems.

EXPERIMENTAL

Materials

The synthesis of *p*-(hexafluoro-2-hydroxyisopropyl)styrene and its copolymerization with styrene were described previously⁴. (We are indebted to Dr C. H. Do for preparing the monomer and the copolymers.) Three copolymers containing 4.8, 8.1 and 19.7 mol% of the hydroxy moiety, respectively, were used in this study. These modified polystyrenes are designated as MPS5, MPS8 and MPS20. The M_n (polystyrene equivalent) and M_w/M_n values for the three polymers are 40 000 and 2.0, 92 000 and 1.6, and 33 000 and 2.0 respectively. The glass transition temperatures are 101, 104 and 107°C.

Poly(methyl methacrylate) from Scientific Polymer Products has molecular weight values of $M_n = 46 000$ and $M_w/M_n = 2.02$. The glass transition temperature of the sample is 110°C. Two poly(styrene-co-acrylonitrile) samples were used. The number-average molecular weight of PSAN30, also from Scientific Polymer Products, containing 30% by weight of AN, is 81 000 and M_w/M_n is 2.0. The M_n and M_w/M_n values of PSAN19 (from Dow Corp.), containing 18.9% AN, are 112 000 and 1.94. The glass

* To whom correspondence should be addressed

transition temperature of PSAN19 is 106°C, and that of PSAN30 is 107°C.

Preparation of films

Thin films of individual polymers or blends were prepared by solution casting from 2-butanone. The final drying step took place in a vacuum desiccator for one day at about 120°C. This temperature, which was above the T_g for every polymer or blend examined, was chosen to ensure effective removal of residual solvent. Layers of thin films were stacked and pressed in a Carver hot press at 160–165°C to the desired thickness for diffusion experiments.

Glass transition temperatures

The glass transition temperatures of polymers were determined by differential scanning calorimetry, with the use of a DuPont Thermal Analyzer, model 1090. The heating rate for the thermal scan was 10°C min⁻¹, and the midpoint of the jump in specific heat was identified as T_g . The values reported are averages of at least two measurements. The range of uncertainty is about ±1°C.

Specific volume

The specific volume of a polymer was determined at 23°C by using a density gradient column prepared from an aqueous solution of sodium bromide. At least three observations were made for each specimen and the average value was used. The experimental error was about ±0.0005 cm³ g⁻¹. Where literature data are available for comparison, e.g. PMMA, PSAN30 and PSAN19, the agreement with our measurement is within 0.001 cm³ g⁻¹.

Vapour diffusion experiments

The amount of water vapour absorbed by a polymer was measured by the quartz spring method using a cathetometer equipped with a digital linear gauge for height measurement. The temperature of the sorption chamber was controlled to ±0.2°C. Equilibrium water vapour sorption was measured at several partial vapour pressures at each temperature, using the method of successive sorption and desorption. The sensitivity of the measurement was about 2 × 10⁻³ mg. The reproducibility of data was about ±2% when different batches of films were tested.

The sorption kinetics experiments were conducted only

at p/p_0 of 0.5 and 0.9. Following each sorption experiment, a desorption measurement was carried out to see whether sorption–desorption data fell on a single curve. Films of different thicknesses were used to check the superposability of reduced curves (M_t versus $t^{1/2}/l$). The diffusion coefficient was calculated from the slope of the linear portion of the $t^{1/2}$ plot¹⁵ in the usual manner (Figure 1). Duplicate experiments were conducted for each material and the uncertainty in the magnitude of D is less than ±5%.

Since the diffusion coefficients were found to be independent of concentration, the calculation of activation energy of diffusion E_D is straightforward. For several polymers, diffusion coefficients were measured at six temperatures between 26 and 50°C. The correlation coefficients for the Arrhenius plots range from 0.970 to 0.996. For others, diffusion data were collected only at 30 and 50°C. The uncertainty in E_D values is estimated to be ±8%.

RESULTS

The specific volume, equilibrium water absorption, diffusion coefficient and activation energy of diffusion of the six component polymers and 30 blends are summarized in Tables 1–5. The relation between chemical structure and each of the above quantities will be described below.

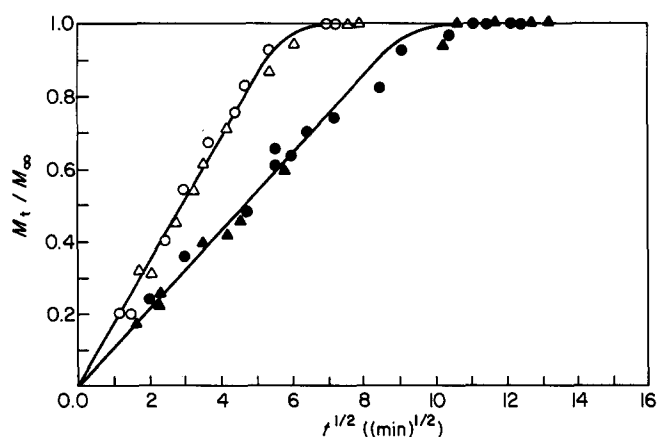


Figure 1 Water vapour sorption curve of PMMA: (●) sorption and (▲) desorption at 30°C; (○) sorption and (△) desorption at 50°C

Table 1 Summary of data for PMMA, PSAN and MPS

	PMMA	PSAN19	PSAN30	MPS5	MPS8	MPS20
$V(23^\circ\text{C})$ (cm ³ g ⁻¹)	0.8389	0.9363	0.9275	0.9259	0.8945	0.8453
Solubility (26°C, $a_1 = 0.50$)						
$C \times 10^2$ (g g ⁻¹)	0.750	0.255	0.370	0.150	0.260	0.401
$S \times 10^2$ (cm ³ cm ⁻³)	0.891	0.271	0.398	0.162	0.290	0.473
$D \times 10^8$ (cm ² s ⁻¹)						
30°C	1.53	15.0	6.02	18.4	11.0	7.15
50°C	3.92	30.8	13.6	40.0	30.0	18.2
E_D (kcal mol ⁻¹)	10.0	7.1	7.5	7.6	8.9	9.2
$D_0 \times 10^3$ (cm ² s ⁻¹)	213	17.2	15.2	54.7	289	262
ΔS^* (cal K ⁻¹ mol ⁻¹)	4.6	-0.47	0.71	1.9	52	5.0
$V(T) - V_0(0)$ (cm ³ g ⁻¹)	0.109	0.153	0.145	0.165	0.152	0.151

Specific volume

The specific volumes of PMMA, PSAN19 and PSAN30 determined in our experiments agree well with literature values. In PSAN polymers, a linear decrease

of specific volume V with increasing nitrile content has been documented¹¹. In a similar way, the specific volume of an MPS polymer decreases as the amount of hexafluoro-2-hydroxyisopropyl group increases, but the relation is not linear.

When the specific volumes of blends are compared with the weight-average values of the component polymers ($W_1V_1 + W_2V_2$), the excess volumes V^e are close to zero in three blends, slightly negative in two and positive in four. Belonging to the first category are PMMA/PSAN30, PMMA/MPS5 and PSAN30/MPS8; to the second, PSAN19/MPS5 and PSAN30/MPS5. The four blends that show positive excess volumes are PMMA/MPS8, PMMA/MPS20, PSAN19/MPS8 and PSAN30/MPS20. A qualitative ranking of the magnitude of V^e is given in Table 6, and representative data for each type of behaviour are shown in Figure 2. We note that positive excess volume is a rare event in miscible blends. To our knowledge, there is only one recent publication reporting positive excess volumes¹⁶.

Solubility

The equilibrium sorption or solubility C at 26°C in each of the 36 polymers is small even at high vapour

Table 2 Summary of data for PMMA/PSAN30 blends

	PSAN30 (wt%)		
	25	50	75
$V(23^\circ\text{C})$ ($\text{cm}^3 \text{g}^{-1}$)	0.8613	0.8857	0.9124
Solubility (26°C, $a_1 = 0.50$)			
$C \times 10^2$ (g g^{-1})	0.611	0.518	0.431
$S \times 10^2$ ($\text{cm}^3 \text{cm}^{-3}$)	0.707	0.583	0.471
$D \times 10^8$ ($\text{cm}^2 \text{s}^{-1}$)			
30°C	2.31	3.32	5.39
50°C	6.18	7.72	11.9
E_D (kcal mol^{-1})	9.5	8.4	7.8
$D_0 \times 10^3$ ($\text{cm}^2 \text{s}^{-1}$)	149	34.6	22.9
ΔS^* ($\text{cal K}^{-1} \text{mol}^{-1}$)	3.8	0.94	0.11
χ_{12}	-0.05	0	-0.17
$V(T) - V_0(0)$ ($\text{cm}^3 \text{g}^{-1}$)	0.116	0.127	0.147

Table 3 Summary of data for PMMA/MPS blends

	MPS5 (wt%)			MPS8 (wt%)			MPS20 (wt%)		
	25	50	75	25	50	75	25	50	75
$V(23^\circ\text{C})$ ($\text{cm}^3 \text{g}^{-1}$)	0.8599	0.8818	0.9033	0.8547	0.8696	0.8826	0.8432	0.8475	0.8467
Solubility (26°C, $a_1 = 0.50$)									
$C \times 10^2$ (g g^{-1})	0.480	0.312	0.218	0.450	0.341	0.280	0.492	0.409	0.370
$S \times 10^2$ ($\text{cm}^3 \text{cm}^{-3}$)	0.556	0.343	0.241	0.525	0.391	0.316	0.581	0.478	0.436
$D \times 10^8$ ($\text{cm}^2 \text{s}^{-1}$)									
30°C	3.76	8.24	11.8	3.20	4.30	7.78	3.82	6.29	7.47
50°C	9.65	20.0	27.5	7.36	10.2	16.3	6.82	10.2	13.7
E_D (kcal mol^{-1})	9.2	8.7	8.3	8.0	7.7	7.5	5.7	4.7	6.0
$D_0 \times 10^3$ ($\text{cm}^2 \text{s}^{-1}$)	157	141	105	15.2	14.5	18.5	0.449	0.157	1.37
ΔS^* ($\text{cal K}^{-1} \text{mol}^{-1}$)	4.0	3.7	3.2	-0.71	-0.81	-0.32	-7.8	-9.9	-5.5
χ_{12}	-0.05	-0.08	0	-1.2	-0.96	-0.99	-1.4	-1.2	-1.2
$V(T) - V_0(0)$ ($\text{cm}^3 \text{g}^{-1}$)	0.124	0.139	0.152	0.120	0.134	0.140	0.123	0.139	0.148

Table 4 Summary of data for PSAN19/MPS blends

	MPS5 (wt%)			MPS8 (wt%)			MPS20 (wt%)		
	25	50	75	25	50	75	25	50	75
$V(23^\circ\text{C})$ ($\text{cm}^3 \text{g}^{-1}$)	0.9320	0.9285	0.9268	0.9268	0.9183	0.9066	0.9183	0.8985	0.8726
Solubility (26°C, $a_1 = 0.50$)									
$C \times 10^2$ (g g^{-1})	0.220	0.195	0.170	0.220	0.195	0.235	0.239	0.248	0.289
$S \times 10^2$ ($\text{cm}^3 \text{cm}^{-3}$)	0.235	0.209	0.183	0.237	0.212	0.258	0.259	0.275	0.349
$D \times 10^8$ ($\text{cm}^2 \text{s}^{-1}$)									
30°C	16.8	20.2	19.5	17.0	18.5	14.7	17.2	16.6	12.2
50°C	34.8	41.0	40.0	31.4	33.4	30.0	28.0	25.1	22.0
E_D (kcal mol^{-1})	7.1	6.9	7.1	6.0	5.8	7.0	4.8	4.1	5.9
$D_0 \times 10^3$ ($\text{cm}^2 \text{s}^{-1}$)	22.0	19.0	22.0	3.50	2.61	15.2	0.450	0.133	2.17
ΔS^* ($\text{cal K}^{-1} \text{mol}^{-1}$)	0.0	-0.27	0.0	-3.7	-4.2	-0.70	-7.7	-10.2	-4.6
χ_{12}	-0.05	0	-0.05	-0.82	-0.72	-0.52	-0.96	-0.96	-0.71
$V(T) - V_0(0)$ ($\text{cm}^3 \text{g}^{-1}$)	0.156	0.158	0.161	0.154	0.156	0.154	0.161	0.160	0.155

Table 5 Summary of data for PSAN30/MPS blends

	MPS5 (wt%)			MPS8 (wt%)			MPS20 (wt%)		
	25	50	75	25	50	75	25	50	75
$V(23^\circ\text{C})$ ($\text{cm}^3 \text{g}^{-1}$)	0.9259	0.9242	0.9251	0.9191	0.9090	0.9025	0.9115	0.8920	0.8703
Solubility (26°C , $a_1 = 0.50$)									
$C \times 10^2$ (g g^{-1})	0.268	0.210	0.177	0.337	0.305	0.280	0.301	0.275	0.315
$S \times 10^2$ ($\text{cm}^3 \text{cm}^{-3}$)	0.289	0.227	0.191	0.366	0.335	0.309	0.329	0.307	0.361
$D \times 10^8$ ($\text{cm}^2 \text{s}^{-1}$)									
30°C	7.91	9.90	12.9	7.37	8.26	9.87	8.42	10.3	9.00
50°C	17.7	23.3	29.7	16.3	18.9	23.0	15.7	17.4	17.8
E_D (kcal mol^{-1})	7.9	8.4	8.2	7.8	8.1	8.3	6.1	5.1	6.7
$D_0 \times 10^3$ ($\text{cm}^2 \text{s}^{-1}$)	35.7	102	93.8	27.7	54.4	87.4	2.01	0.50	5.60
ΔS^* ($\text{cal K}^{-1} \text{mol}^{-1}$)	1.0	3.1	2.9	0.49	1.8	2.8	-4.8	-7.6	-2.7
χ_{12}	-0.48	-0.44	-0.32	-0.05	-0.08	-0.16	-1.29	-0.96	-1.12
$V(T) - V_0(0)$ ($\text{cm}^3 \text{g}^{-1}$)	0.149	0.155	0.160	0.146	0.146	0.150	0.154	0.158	0.156

Table 6 Summary of the sign and relative magnitude of the 'excess' properties for each blend system

Blends	V^e	$E_D - (\phi_1 E_{D1} + \phi_2 E_{D2})$	$\ln D - (\phi_1 \ln D_1 + \phi_2 \ln D_2)$		
			30°C	50°C	S^e
1. PMMA/PSAN30	~0	~0	~0	~0	s(-)
2. PMMA/MPS5	0	0	m(+)	m(+)	vs(-)
3. PMMA/MPS8	s(+)	l(-)	s(+)	~0	l(-)
4. PMMA/MPS20	l(+)	vl(-)	vl(+)	s(+)	l(-)
5. PSAN19/MPS5	s(-)	s(-)	m(+)	s(+)	vs(-)
6. PSAN19/MPS8	s(+)	l(-)	s(+)	~0	l(-)
7. PSAN19/MPS20	l(+)	vl(-)	l(+)	~0	l(-)
8. PSAN30/MPS5	s(-)	m(+)	vs(-)	0	m(-)
9. PSAN30/MPS8	~0	0	0	0	vs(-)
10. PSAN30/MPS20	l(+)	l(-)	vl(+)	s(+)	l(-)

vs = very small, s = small, m = medium, l = large, vl = very large

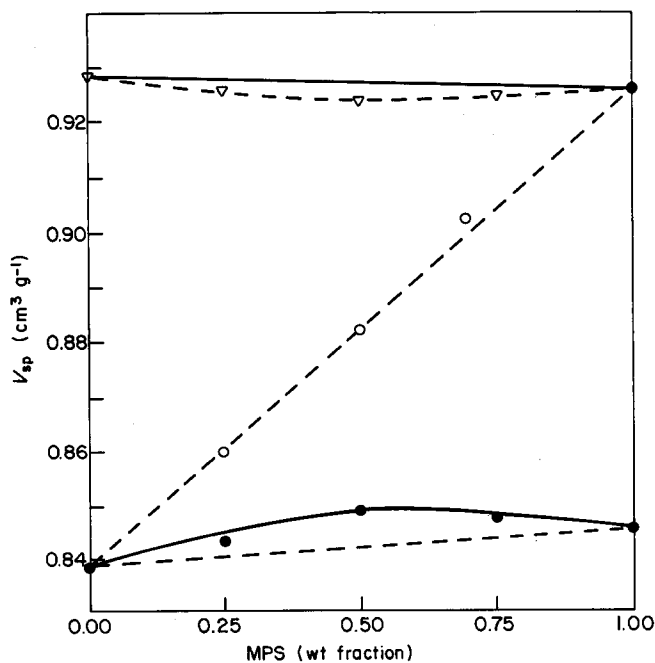


Figure 2 Specific volumes of representative polymer blends: (○) PMMA/MPS5; (●) PMMA/MPS20; (▽) PSAN30/MPS5

pressures. Only in PMMA and one of its blends does solubility exceed 0.01 g g^{-1} at a relative pressure p/p_0 of 0.9. As in the case of many other polymers with low water solubility, all sorption isotherms are linear up to p/p_0 of 0.6–0.7. At higher vapour pressures, deviations from linearity occur. However, the deviations are small even at p/p_0 of 0.9 and exceed 10% of the value calculated from linear extrapolation only in four cases. For the purpose of comparison, solubility values at 26°C and $p/p_0 = 0.5$ will be used because there is no doubt about the linearity of the sorption isotherms up to that pressure.

The solubilities for the component polymers are summarized in Table 1. The value for PMMA is $0.75 \times 10^{-2} \text{ g g}^{-1}$, in good agreement with literature^{17–20}. The solubilities in PSAN and MPS polymers range from 0.15×10^{-2} to $0.40 \times 10^{-2} \text{ g g}^{-1}$. These values are 5–12 times larger than the reported solubility of about $0.033 \times 10^{-2} \text{ g g}^{-1}$ in polystyrene²¹. The data in Table 1 show a clear trend of increasing solubility with increasing polar group content in styrene copolymers. The hydroxy groups appear to be more effective in raising water vapour solubility than the nitrile group when comparison is made on a molar basis.

When the solubility in a blend (Tables 2–5), expressed in g g^{-1} , is compared with the solubilities in the

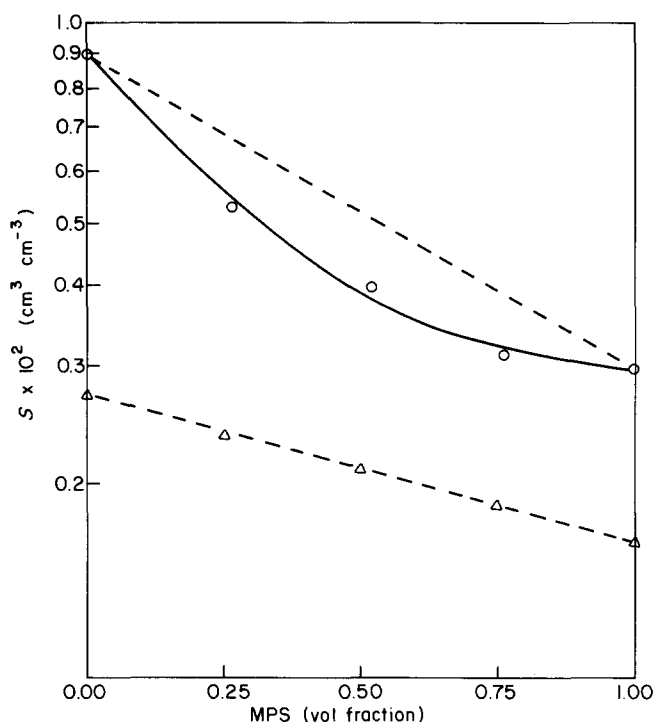


Figure 3 Solubility of water vapour in representative polymer blends: (Δ) PSAN19/MPS5; (\circ) PMMA/MPS8

component polymers, the former is either nearly equal to or smaller than the average value for the components. The analysis of the experimental data to be described later, however, calls for solubilities expressed as volume fractions. Therefore, the quantities S , expressed in $\text{cm}^3 \text{H}_2\text{O}/\text{cm}^3 \text{polymer}$ ($\text{cm}^3 \text{cm}^{-3}$), are also given in the tables. The excess solubility, defined as $(S - \phi_1 S_1 - \phi_2 S_2)$, where ϕ_1 and ϕ_2 represent the volume fractions of the component polymers in the blend, is always negative. In one group of blends, namely PMMA/PSAN30, PMMA/MPS5, PSAN19/MPS5 and PSAN30/MPS8, excess solubilities have very small negative values. In the second group, the values are much more negative. Blends of PMMA/MPS8, PMMA/MPS20, PSAN19/MPS8, PSAN19/MPS20, PSAN30/MPS8 and PSAN30/MPS20 belong to the second category. One example for each group is shown in Figure 3. The relative magnitudes of excess solubility S^e are also ranked in Table 6.

Diffusion coefficient

The diffusion coefficients D of water vapour in the six component polymers are listed in Table 1. The value for PMMA at 30°C is $1.5 \times 10^{-8} \text{cm}^2 \text{s}^{-1}$; it increases to $3.9 \times 10^{-8} \text{cm}^2 \text{s}^{-1}$ at 50°C . Our results are comparable to other studies using the sorption kinetics method. The primary difference between our data and earlier investigations concerns the concentration dependence of D reported by some authors but not found in the present work. In refs 17–19, D was regarded as a constant of $(4\text{--}5) \times 10^{-8} \text{cm}^2 \text{s}^{-1}$, close to our value at 50°C .

The diffusion coefficients in PSAN and MPS polymers range from 6×10^{-8} to $18 \times 10^{-8} \text{cm}^2 \text{s}^{-1}$ at 30°C . These values are smaller than the diffusion coefficient in PS of about $30 \times 10^{-8} \text{cm}^2 \text{s}^{-1}$, estimated from permeability coefficient and solubility at 25°C ²¹. The decrease in diffusion coefficient upon increasing polar group content is opposite to the trend in solubility behaviour. When the data for PSAN are compared with those for MPS,

the hydroxy group is seen to be more effective in reducing D than the nitrile group.

The diffusion coefficients in the blends, when compared with the corresponding average D values ($\phi_2 D_1 + \phi_1 D_2$) fall into two categories. In the first group, D_{blend} is represented very closely by the average values; blends of PMMA/PSAN30, PMMA/MPS8, PSAN30/MPS5 and PSAN30/MPS8 belong in this group. In the second group, which includes the rest of the blends, $D_{\text{blend}}(30^\circ\text{C})$ exceeds the average value. One example of each type of behaviour is shown in Figure 4. The relative magnitudes of the difference between $\log D_{\text{blend}}$ and $(\phi_1 \log D_1 + \phi_2 \log D_2)$ are also ranked in a qualitative manner in Table 6. Note that, while the deviations are positive at 30°C for PSAN19/MPS8 and PSAN19/MPS20, the differences become almost zero at 50°C . The reason for this will be explained in later discussion.

Activation energy

The activation energy for diffusion of water vapour in PMMA was determined to be $E_D = 10 \text{kcal mol}^{-1}$, which is comparable to literature values. For PSAN and MPS polymers, there is a small increase in activation energy E_D as nitrile or hydroxy content increases (Table 1).

In each of the three blend systems, PMMA/PSAN30, PMMA/MPS5 and PSAN30/MPS8, the difference between the experimental E_D and the average value ($\phi_1 E_{D1} + \phi_2 E_{D2}$) is negligible. The differences are negative in six blends, namely PMMA/MPS8, PMMA/MPS20, three PSAN19 blends and PSAN30/MPS20. Only in one blend system, PSAN30/MPS5, is the difference positive. The relative magnitudes of $(E_D - \phi_1 E_{D1} - \phi_2 E_{D2})$ are summarized in Table 6, and examples of the three types of E_D behaviours are shown in Figure 5.

In the studies of gas diffusion in polymers, there is a well established linear correlation between $\ln D_0$ and

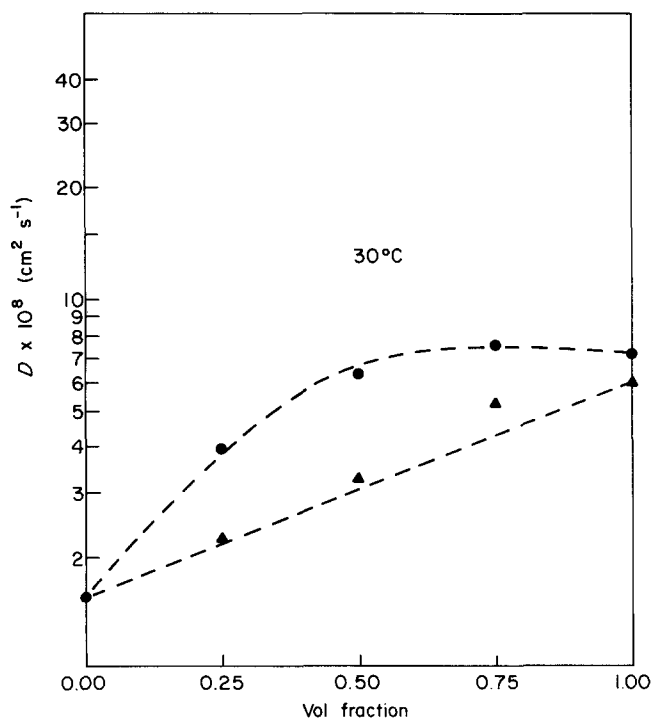


Figure 4 Representative diffusion coefficients in polymer blends at 30°C : (\blacktriangle) PMMA/PSAN30; (\bullet) PMMA/MPS20

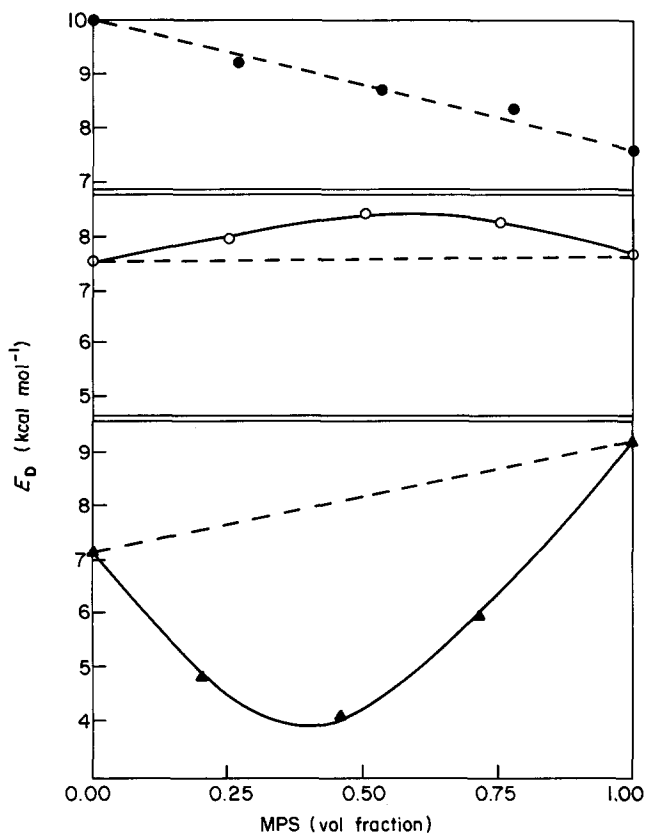


Figure 5 Excess activation energies: (●) PMMA/MPS5; (○) PSAN30/MPS5; (▲) PSAN19/MPS20

E_D/T , where D_0 is the pre-exponential term in the Arrhenius equation^{22,23}. Our $\ln D_0$ and E_D values conform to a similar linear correlation (Figure 6); however, the straight line is shifted from the data of Barrer and Skirrow²².

The entropy of activation ΔS^* in Eyring's activated state theory can be calculated from D_0 if a reasonable value of jump distance λ is assumed¹⁵. In the present calculation, a value of 3.5 Å for λ and an average temperature of 313 K are used. A plot of ΔS^* versus E_D is shown in Figure 7. Note that ΔS^* values are negative in many blends. The choice of a smaller λ value of 1.5 Å still does not change the sign of ΔS^* to positive in most cases. Though seldom reported in the literature, negative ΔS^* values were found for gas diffusion in poly(dimethylsiloxane) (PDMS)²³. Together with low activation energies, the negative ΔS^* values were thought to be associated with the flexibility of the PDMS chain. However, the explanation is inapplicable to our polymers. Rather than interpreting negative ΔS^* values as indicative of constrained transition states, we believe that, in the context of the study, ΔS^* values reflect, on a comparative basis, the number of degrees of freedom involved in the cooperative motion of segments. A full explanation will be given later.

DISCUSSION

Information about the state of mixing of polymer blends and segmental mobility can be deduced from specific volume, solubility and diffusion data. The two thermodynamic quantities, S and V , will be discussed first.

Polymer-polymer interaction from solubility measurements

Polymer-polymer interaction parameter χ_{12} can be calculated from equilibrium sorption as follows. The Flory-Huggins (FH) equation applied to polymer-solvent mixtures containing very small amounts of the solvent is approximated by:

$$a_s/S = \exp(1 + \chi) \quad (1)$$

where a_s is the activity of the solvent and χ is the solvent-polymer interaction parameter²⁴. Extension of FH

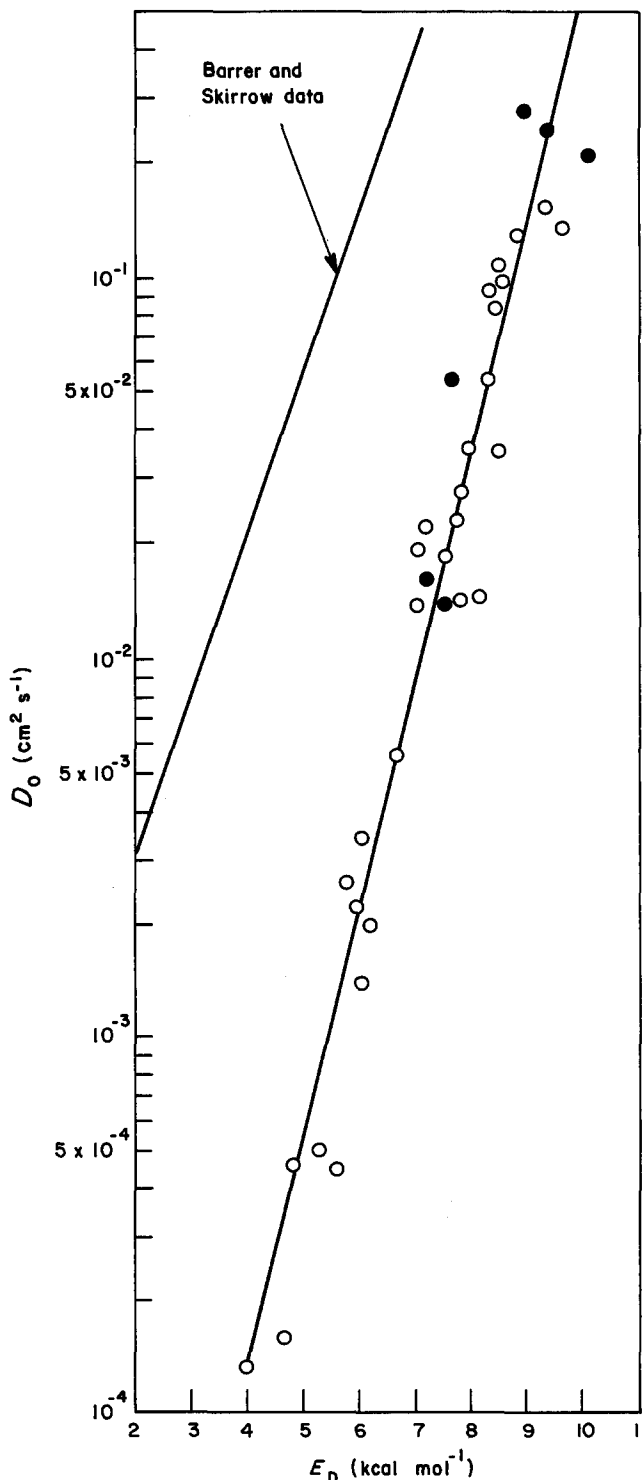


Figure 6 Relationship between $\ln D_0$ and E_D

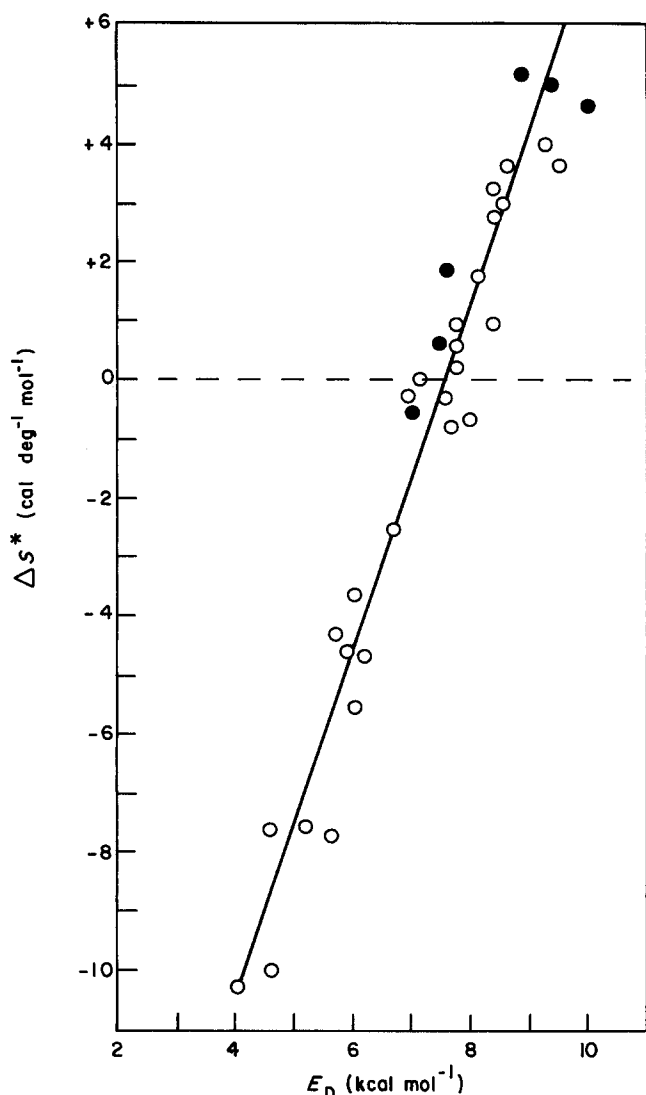


Figure 7 Relationship between activation entropy and activation energy

theory to ternary mixtures²⁵ results in:

$$\chi_{12} = (\chi - \phi_1\chi_1 - \phi_2\chi_2)/\phi_1\phi_2 \quad (2)$$

For solubilities measured at the same solvent activity, 0.5 in our case, the following equation provides a direct method of calculating χ_{12} :

$$\ln S = \phi_1 \ln S_1 + \phi_2 \ln S_2 + \chi_{12}\phi_1\phi_2 \quad (3)$$

The limitation of the above method lies in the large error incurred in the calculation of a small $\chi_{12}\phi_1\phi_2$ term as the difference between three large quantities. A more serious reservation concerns the legitimacy of using a mean-field calculation for blends in which specific interaction plays a dominant role. Recently, Sanchez and Balazs²⁶ generalized the lattice fluid model to take into account AB-type specific interactions. Painter and Coleman²⁷, on the other hand, appended to the Flory-Huggins equation a term that described the free-energy changes related to hydrogen bonding between components of binary polymer blends. We did not apply these theories because many of the parameters necessary for carrying out the calculations were unavailable. Thus, while acknowledging that the χ values listed in Tables 2-5 are vulnerable to criticism on theoretical grounds, we nevertheless believe that they are useful for detecting trends as blend compositions change.

The χ_{12} values for PMMA/PSAN30 blends range from 0 to -0.17 , which, as will be seen later, are to be considered as small negative values in the present context. The PMMA/PSAN30 is a typical example for which the copolymer effect is operative. For blends of homopolymer A with copolymer BC, theory predicts that χ_{blend} may become negative for a certain range of copolymer compositions even though all three binary interaction parameters χ_{AB} , χ_{AC} and χ_{BC} are positive. From the range of miscible copolymer compositions, called miscibility window, the binary interaction parameters for MMA/S, MMA/AN and S/AN have been estimated by Paul¹¹ and by Cowie and Lath²⁸. Using Paul's estimates, χ_{12} for PMMA/PSAN30 is computed to be about -0.014 .

Small negative χ_{12} values, 0 to -0.008 , are also computed for PMMA/MPS5 blends from solubility data. In this homopolymer-copolymer combination, one of the binary interaction parameters is negative due to hydrogen-bonding interaction and certainly contributes to the negative sign of χ_{12} . As hydroxy content in MPS increases, it is expected that χ_{12} values for PMMA/MPS8 and PMMA/MPS20 become progressively more negative. Indeed, experimental χ_{12} values are -0.96 to -1.2 for PMMA/MPS8 and -1.2 to -1.4 for PMMA/MPS20 blends.

Blends of PSAN and MPS contain two copolymers that share a common monomer. Again, χ_{12} is composed of three binary interaction parameters. As in PMMA/MPS blends, χ_{12} values for PSAN19/MPS blends become more negative as HHIS content in MPS increases. The computed χ_{12} values for the two blend systems are comparable in magnitude.

The data for PSAN30/MPS8 blends are out of place from the others in the series. The computed χ_{12} values are less negative than those for PSAN30/MPS5. With MPS20, large negative values are again obtained. We have no explanation for the trend reversal.

Specific volume

Before we engage in a discussion of the specific volumes of the blends, it ought to be mentioned that the measurement of specific volume in the glassy state is complicated by the phenomenon of volume relaxation. In our experiments, densities were measured after films had been stored for at least several days. We did not take precautions to ensure the same thermal histories for all samples. Even if we did, the relaxation rates may be different for the constituent polymers and their blends^{29,30}. Strictly speaking, the volume measurements are not necessarily comparable. However, the relaxation rate²⁹ (enthalpy) of PMMA/PSAN30 was found to be already slow at $T_g - 50^\circ\text{C}$; at $T_g - 90^\circ\text{C}$ during the storage of our specimens, volume relaxation rates are expected to be even slower. Experimentally, duplicate density measurements performed for several (not all) films at different time intervals showed no differences.

Excess volume is a useful indicator of the change in chain packing in the blends compared to the component polymers. The excess volumes for a number of PMMA/PSAN blends have been reported to be zero within experimental accuracy and suggest relatively weak interactions. Our V^e and χ_{12} data for PMMA/PSAN30 agree with that interpretation. It seems reasonable to conclude that there is essentially no change in the state of chain packing of each component polymer upon blending. Two

other blends, PMMA/MPS5 and PSAN30/MPS8, also have zero excess volumes and small negative χ_{12} values.

Both PSAN19/MPS5 and PSAN30/MPS5 blends have small negative excess volumes, about -0.0012 to $-0.0026 \text{ cm}^3 \text{ g}^{-1}$. The former blends have small negative χ_{12} values, while for the latter the interaction parameters are significantly more negative. However, there does not appear to be a quantitative relation between the magnitudes of excess volume and χ_{12} .

Unexpectedly, the remaining five blend systems have positive excess volumes. Recent literature recorded at least 15 miscible polymer blends as having zero or negative excess volumes. Only a single pair, PMMA/poly(vinylidene fluoride)¹⁶, was reported to have a positive excess volume. The authors concluded from calculations using Flory's equation-of-state theory that certain combinations of reduced pressures, reduced temperatures and exchange interaction could indeed result in positive excess volumes. However, our discussion will be based on the effect of chemical structure on chain packing.

Infra-red spectra of MPS polymers show the hydroxy groups present in both 'free' and 'self-associated' states⁴. At low hydroxy contents, e.g. 5%, the absorption peak at 3600 cm^{-1} due to free hydroxy groups is strong while the broad peak at 3520 cm^{-1} due to self-associated hydroxy groups is very weak. As hydroxy content increases, the absorption of the self-associated species increases in intensity. The intensities of both absorptions decrease drastically in PMMA blends. The decreases are accompanied by the emergence of a new peak at 3400 cm^{-1} , indicative of hydroxy groups⁷ bonded to carbonyl groups. The important point to be made here is that carbonyl groups interact with both free and self-associated hydroxy groups; the latter case involves an exchange of hydrogen bonding.

The spectroscopic observations form the basis of interpretation of our volume data. Central to our interpretation is the assumption that volume shrinkage to be expected from the formation of a hydrogen bond between a free hydroxy group and a carbonyl group is countered by poor packing of the inherently immiscible units of styrene and methyl methacrylate in the vicinity of the interaction site. Consequently, the net volume change is very small. When an exchange of hydrogen bonds takes place between self-associated hydroxy groups and carbonyl groups, the combined effect of break-up of self-association and local repulsion between styrene and MMA units is now sufficient to cause a net increase in volume. As hydroxy content increases in MPS, the fraction of self-associated species increases. Since both the free and the self-associated hydroxy groups form hydrogen bonds with carbonyl groups⁴, it is to be expected that excess volume becomes progressively more positive as hydroxy content increases.

The excess volumes of PSAN/MPS blends increase from slightly negative to progressively positive values as hydroxy contents increase in MPS. The trend of the increase is similar to that in PMMA/MPS blends. But a point of difference in interpretation is worthy of note. The two copolymers share a common monomer unit, namely styrene. Thus, chain packing is expected to pose a less severe problem in these blends; only the repulsion between styrene and acrylonitrile units needs to be considered. In the blends of MPS5 with PSAN19 or PSAN30, volume contraction due to hydrogen-bond

formation between hydroxy and nitrile groups wins against local repulsion between styrene units in MPS and AN units in PSAN, resulting in slightly negative excess volumes. Note that styrene and AN units in PSAN, although chemically linked, also 'dislike' each other. In blends of MPS8 and MPS20, again the excess volumes increase to positive values for the reasons given above.

Another potential cause for positive excess volume, though inapplicable to the blends used in this study, deserves brief mention. When blends are formed from strongly interacting pairs, the glass transition temperatures of the blends are frequently much higher than the average T_g values of the component polymers. In these systems, it is possible that a larger than expected volume is frozen-in at T_g of the blend. However, all our component polymers have similar T_g values, between 101 and 110°C , and the values for the blends are within 2°C of the respective average T_g values of the components. Accordingly, we believe that such an effect is unimportant in this investigation.

Diffusion coefficient

We now turn our attention to segmental mobility in blends as perceived by water vapour in its role as a diffusional probe. Equations derived by Paul will be used below. As mentioned earlier, $\ln D_0$ and E_D in the Arrhenius equation have been found to be linearly related in a large body of gas diffusion data. Our results are represented by a similar linear relationship. If the slope of the linear plot is b , the diffusion coefficient D in a blend can be expressed⁹ by:

$$\ln D = \ln D_1 + \phi_2 \ln D_2 + (bRT - 1)\Delta E_{12}/RT \quad (4)$$

where $(bRT - 1)$ is negative, about -0.5 , and ΔE_{12} is defined as:

$$\Delta E_{12} = E_D - (\phi_1 E_{D1} + \phi_2 E_{D2}) \quad (5)$$

For convenience, let $\Delta \ln D$ represent the difference between $\ln D$ and $(\phi_1 \ln D_1 + \phi_2 \ln D_2)$. According to equation (4), $\Delta \ln D$ and ΔE_{12} must have opposite signs because $(bRT - 1)$ is negative. An inspection of the relative magnitudes of $\Delta \ln D$ in Table 6 shows that the quantity $\Delta \ln D$ is either positive or very close to zero. Therefore, ΔE_{12} is expected to be negative or near zero. The prediction is obeyed in all except possibly one blend system; in PMMA/MPS5 blends, $\Delta \ln D$ is positive but ΔE_{12} is near zero. Even if the exception is disregarded, quantitative correlation between $\Delta \ln D$ and ΔE_{12} is not obtained.

In the course of analysing our data by equation (4), it came upon us that the magnitudes of $\Delta \ln D$ at 30 and 50°C were significantly different in several blends. This is the result of different activation energies for the component polymers and blends. Therefore it is desirable to conduct experiments over a wide range of temperatures when equation (4) is used to analyse diffusion data.

Correlation between ΔE_{12} and excess volume

Since activation energy is expended to create a hole of sufficient size for a diffusional jump, it is thought that ΔE_{12} may bear a direct relation with excess volume. In seeking such a correlation, we plotted $\Delta E_{12}/E_D(\text{calc})$ against $V^e/V(\text{calc})$ where $E_D(\text{calc})$ is $(\phi_1 E_{D1} + \phi_2 E_{D2})$ and $V(\text{calc})$ is $(W_1 V_1 + W_2 V_2)$. The plot is shown in Figure 8. Although there is scatter in the data, the trend

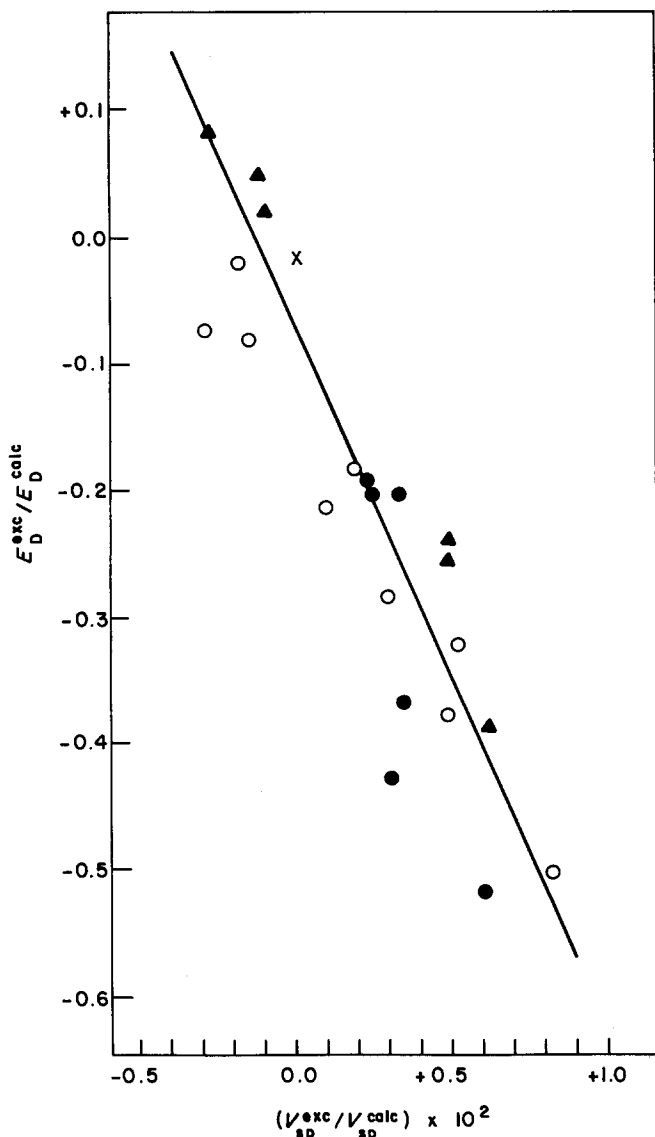


Figure 8 Correlation between excess activation energy and excess volume

is clear. Negative ΔE_{12} values are associated generally with positive excess volumes, while the three positive ΔE_{12} values are located in the region of negative excess volumes. It follows from the relationship between $\Delta \ln D$ and ΔE_{12} that $\Delta \ln D$ and V^e should have the same sign. This is indeed the case except for PSAN19/MSP5.

It is of interest to note that negative entropies of activation go hand in hand with negative ΔE_{12} or positive excess volume (with one exception). Apparently, the positive excess volumes in these blends decrease the number of segments needed for cooperative motion in a diffusion jump, resulting in small values of ΔS^* on a comparative basis.

Free volume

In the free-volume theory of diffusion³¹, the diffusion coefficient can be expressed by:

$$D = A \exp(-V^*/v_f) \tag{6}$$

where v_f is the average size of the free volume and V^* is the critical hole size for the diffusional jump. A numerical factor between 0.5 and 1 for V^* is omitted here for the sake of clarity. Although the free-volume theory was applied most frequently to experiments above T_g , the use

of equation (6) to analyse diffusion data below T_g is presented below.

The temperature dependence of v_f below T_g may be represented by:

$$v_f = v_f(T_r) + \alpha(T - T_r) \tag{7}$$

where T_r is a reference temperature and α is the thermal expansion coefficient of free volume in the glassy state. Combination of equations (6) and (7) yields:

$$\frac{1}{\ln(D_T/D_{T_r})} = \frac{[v_f(T_r)]^2}{\alpha V^*} \frac{1}{(T - T_r)} + \frac{v_f(T_r)}{V^*} \tag{8}$$

According to equation (8), a plot of $[\ln(D_T/D_{T_r})]^{-1}$ versus $1/(T - T_r)$ should result in a straight line with an intercept of $v_f(T_r)/V^*$, which is the quantity of interest.

In constructing such plots using 30°C as the reference temperature, it became apparent that even small inaccuracies in experimental D values caused large scatter in the calculated values of $[\ln(D_T/D_{T_r})]^{-1}$. However, straight lines with correlation coefficients greater than 0.994 were obtained when D values from smoothed D versus T curves were used. The quantity $v_f(T_r)/V^*$ from the intercept provides a relative measure of the average

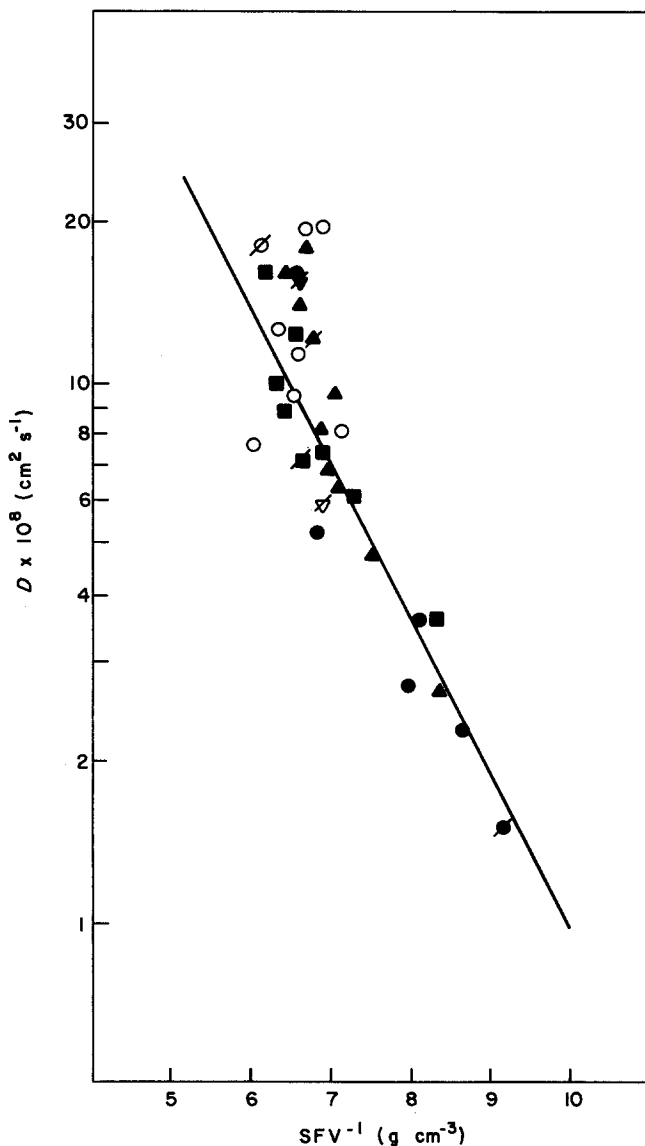


Figure 9 Correlation of diffusion coefficient with specific free volume

Table 7 Values of v_f/V^* for selected polymers

PMMA	MPS8	MPS8 (wt%) in PMMA blends			PSAN30	PSAN30 (wt%) in PMMA blends	
		25	50	75		25	50
0.12	0.04	0.10	0.07	0.05	0.04	0.07	0.06

free volume of each polymer because V^* can be considered to be a constant for a given diffusant. The v_f/V^* values for PMMA, MPS8, PSAN30 and their blends are given in Table 7. Without placing undue emphasis on the significance of their magnitudes, it can nevertheless be said that MPS8 and PSAN30 have about the same v_f while PMMA has a higher value. The computed v_f/V^* values for the blends seem to fall in between those of the component polymers. It should be said, however, that experimental data of high accuracy are needed for a more vigorous test of the above procedure.

In a series of publications by Lee³² and by Paul³³⁻³⁵, it was shown that the permeabilities of a gas through different polymers can be correlated with the 'specific' free volume (SFV) of the polymers by an equation similar in form to equation (6):

$$P = A' \exp\{-B/[V(T) - V_0(0)]\} \quad (9)$$

The specific free volume was defined as $[V(T) - V_0(0)]$, where $V(T)$ is the specific volume of the polymer at temperature T and $V_0(0)$ the occupied specific volume at 0 K. The latter was approximated as 1.3 times the van der Waals volume, according to Bondi³⁶. Our permeability coefficients, calculated from D and S , vary by only a factor of 3 and the validity of the correlation is questionable due to large scatter of the data. However, the 13-fold range of D affords a good correlation between $\ln D$ and $[V(T) - V_0(0)]^{-1}$ as can be seen in Figure 9. The values of B and A' were determined to be 0.66 g cm^{-3} and $1.18 \times 10^8 \text{ cm}^2 \text{ s}^{-1}$ respectively. The correlation suggests the possibility of estimating the water diffusion coefficient of a polymer simply from a knowledge of the specific free volume.

Lastly, it ought to be mentioned that the positive deviation of $\ln D$ from its average value is predicted by the free-volume theory if the free volumes of the constituent polymers are assumed to obey the additivity rule in the blends³⁷.

CONCLUSIONS

The interaction parameters calculated from solubility data are negative for all pairs. As hydroxy content in MPS increases, the interaction parameter tends to become more negative.

In several blends, excess volumes are near zero or slightly negative. In others, the positive excess volumes are believed to reflect poor chain packing in the blend of the inherently immiscible segments of styrene and methyl methacrylate or acrylonitrile.

The deviation of $\ln D$ from its average value is opposite in sign to the deviation of activation energy. The latter bears a direct relation to excess volume.

An excellent correlation was found between D and specific free volume. Analysis of the diffusion data with use of the free-volume theory allows for an estimate of

the ratio of the average free volume to the critical hole size for a diffusional jump.

ACKNOWLEDGEMENT

Support of this work by the National Science Foundation, Division of Materials Research, Grant Number 8820046 is gratefully acknowledged.

REFERENCES

- Kambour, R. P., Bendler, J. T. and Bopp, R. C. *Macromolecules* 1983, **16**, 753
- tenBrinke, G., Karasz, F. E. and MacKnight, W. J. *Macromolecules* 1983, **16**, 1827
- Paul, D. R. and Barlow, J. W. *Polymer* 1984, **25**, 487
- Pearce, E. M., Kwei, T. K. and Min, B. Y. *J. Macromol. Sci., Chem. (A)* 1984, **21**, 1181
- Chen, C. T. and Morawetz, H. *Macromolecules* 1989, **22**, 159
- Prud'homme, R. E. *Polym. Eng. Sci.* 1982, **22**, 90
- Eisenberg, A. and Hara, M. *Macromolecules* 1984, **17**, 1335
- Eisenberg, A. and Smith, P. J. *Polym. Sci., Polym. Lett. Edn* 1983, **21**, 233
- Paul, D. R. and Chiou, J. S. *J. Appl. Polym. Sci.* 1987, **33**, 2935
- Shur, Y. J. and Ranby, B. *J. Macromol. Sci., Phys. (B)* 1977, **14**, 564; *J. Appl. Polym. Sci.* 1976, **20**, 3121
- Nishimoto, M., Keskkula, H. and Paul, D. R. *Polymer* 1989, **30**, 1279
- Suess, M., Kressler, J. and Kammer, H. W. *Polymer* 1987, **28**, 957
- Naito, K., Johnson, G. E., Allara, D. L. and Kwei, T. K. *Macromolecules* 1978, **11**, 1260
- Fowler, M. E., Barlow, J. W. and Paul, D. R. *Polymer* 1987, **28**, 1177
- Crank, J. and Park, G. S. 'Diffusion in Polymers' (Eds J. Crank and G. S. Park), Academic Press, New York, 1968, Ch. 1
- Wolf, M. and Wendorff, J. H. *Polymer* 1989, **30**, 1524
- Beuche, F. *J. Polym. Sci.* 1954, **14**, 414
- Thomas, A. M. *J. Appl. Polym. Sci. (C)* 1965, **10**, 45
- Roussis, P. P. *J. Membrane Sci.* 1983, **15**, 141
- Barrie, J. A. and Platt, B. *J. Polym. Sci. (A)* 1963, **1**, 304
- Barrie, J. A. 'Diffusion in Polymers' (Eds J. Crank and G. S. Park), Academic Press, New York, 1968, Ch. 8
- Barrer, R. M. and Skirrow, G. *J. Polym. Sci.* 1948, **3**, 549
- Barrer, R. M. and Chio, H. T. *J. Polym. Sci. (C)* 1965, No. 10, 'Transport Phenomena in Polymer Films' (Ed. C. A. Kumins), p. 111
- Flory, P. J. 'Principles of Polymer Chemistry', Cornell University Press, Ithaca, NY, 1953
- Scott, R. L. *J. Chem. Phys.* 1949, **17**, 268
- Sanchez, I. C. and Balazs, A. C. *Macromolecules* 1989, **22**, 2325
- Painter, P. C., Park, Y. and Coleman, M. M. *Macromolecules* 1989, **22**, 570
- Cowie, J. M. G. and Lath, D. *Polym. Commun.* 1987, **28**, 300
- Mijovic, J., Ho, T. and Kwei, T. K. *Polym. Eng. Sci.* 1989, **22**, 1604
- Cowie, J. M. G. and Ferguson, R. *Macromolecules* 1989, **22**, 2312
- Cohen, M. H. and Turnbull, D. *J. Chem. Phys.* 1959, **31**, 1164
- Lee, W. M. *Polym. Eng. Sci.* 1980, **20**, 65
- Maeda, Y. and Paul, D. R. *J. Polym. Sci., Polym. Phys. Edn* 1987, **25**, 1005
- Muruganandam, N., Koros, W. J. and Paul, D. R. *J. Polym. Sci., Polym. Phys. Edn* 1987, **25**, 1999
- Barbati, T. A., Koros, W. J. and Paul, D. R. *J. Polym. Sci., Polym. Phys. Edn* 1988, **26**, 709
- Bondi, A. 'Physical Properties of Molecular Crystals, Liquids, and Glasses', Wiley, New York, 1968
- Chiou, J. S. and Paul, D. R. *J. Appl. Polym. Sci.* 1987, **34**, 1037